



ELSEVIER

Available online at [www.sciencedirect.com](http://www.sciencedirect.com)

SCIENCE @ DIRECT®

Physica A 357 (2005) 18–26

PHYSICA A

[www.elsevier.com/locate/physa](http://www.elsevier.com/locate/physa)

## Crackles and instabilities during lung inflation

Adriano M. Alencar<sup>a,b,\*</sup>, Arnab Majumdar<sup>a,b</sup>, Zoltan Hantos<sup>c</sup>,  
Sergey V. Buldyrev<sup>b</sup>, H. Eugene Stanley<sup>b</sup>, Béla Suki<sup>a</sup>

<sup>a</sup>*Department of Biomedical Engineering, Boston University, Boston, MA 02215, USA*

<sup>b</sup>*Center for Polymer Studies and Department of Physics, Boston University, Boston, MA 02215, USA*

<sup>c</sup>*Department of Medical Informatics and Engineering, and Institute of Surgical Research,  
University of Szeged, Hungary*

Available online 23 June 2005

---

### Abstract

In a variety of physico-chemical reactions, the actual process takes place in a reactive zone, called the “active surface”. We define the active surface of the lung as the set of airway segments that are closed but connected to the trachea through an open pathway, which is the interface between closed and open regions in a collapsed lung. To study the active surface and the time interval between consecutive openings, we measured the sound pressure of crackles, associated with the opening of collapsed airway segments in isolated dog lungs, inflating from the collapsed state in 120 s. We analyzed the sequence of crackle amplitudes, inter-crackle intervals, and low frequency energy from acoustic data. The series of spike amplitudes spans two orders of magnitude and the inter-crackle intervals spans over five orders of magnitude. The distribution of spike amplitudes follows a power law for nearly two decades, while the distribution of time intervals between consecutive crackles shows two regimes of power law behavior, where the first region represents crackles coming from avalanches of openings whereas the second region is due to the time intervals between separate avalanches. Using the time interval between measured crackles, we estimated the time evolution of the active surface during lung inflation. In addition, we show that recruitment and instabilities along the pressure–volume curve are associated with airway opening and recruitment. We find a good agreement between the theory of the dynamics of lung inflation and the experimental data

---

\*Corresponding author.

*E-mail address:* [aalencar@hsph.harvard.edu](mailto:aalencar@hsph.harvard.edu) (A.M. Alencar).

which combined with numerical results may prove useful in the clinical diagnosis of lung diseases.

© 2005 Elsevier B.V. All rights reserved.

*Keywords:* Avalanche; Recruitment; Active surface; Cayley; Tree; Invasion percolation

---

## 1. Introduction

The airway tree structure of the mammalian lung is binary and asymmetric [1], and its main function is to conduct air from the atmosphere to the gas exchange region, composed of more than 300 million alveoli or tiny, thin-membraned sacs. Airway closures and reopenings occur often in diseased lungs and are associated with the generation of crackles [2]. Studies of airway closure and opening indicate that during inflation, airways open in avalanches triggered by overcoming a hierarchy of critical opening threshold pressures along the airway tree [3,4]. The time series of crackle events are complex and the distributions of crackle sound amplitudes [5], and the time intervals between consecutive crackles [6,7] follow power laws.

The growth of colloid aggregates, flame fronts, and tumors occur mainly at the “active surface”, defined as the perimeter of the region where growth occurs. The active surface in the lung is defined as the set of all closed branches which are connected to the root of the tree through an open pathway [6]. During the growth of the active surface, acoustic energy is released as audible crackles [6,7]. When the active surface reaches the alveolar region, lung recruitment and pressure–volume instabilities occur [3]. Here we study the amplitude  $S$  of crackles, the time intervals  $\Delta t$  between consecutive crackles and the effect of generation-dependent thresholds on both the active surface and the distribution of  $\Delta t$  [7].

## 2. Crackling sounds in the lung

The internal surface of the lung is lined with a thin liquid film which can undergo a surface-tension-driven fluid-elastic instability, leading to airway closure by the formation of occluding liquid bridges [8,9]. Crackles are believed to be generated in the non-cartilaginous small and medium-sized airways. Pulmonary crackles are short, “explosive”, transient waves, which are among the many lung sounds generated in diseased lungs during breathing [10–12,2]. A crackle consists of an initial acoustic spike corresponding to the rupture of the liquid bridge followed by a damped acoustic ringing.

An example of the time series of sound amplitudes recorded in the main bronchus during slow inflation from the partially degassed state to the total lobe capacity [5,13] is shown in Figs. 1 and 2. In addition to the acoustic measurements, recruitment in the form of discrete volume increments  $\Delta V$  was assessed with a high-sensitivity flowmeter [13]. To illustrate the relation between crackles and flow,

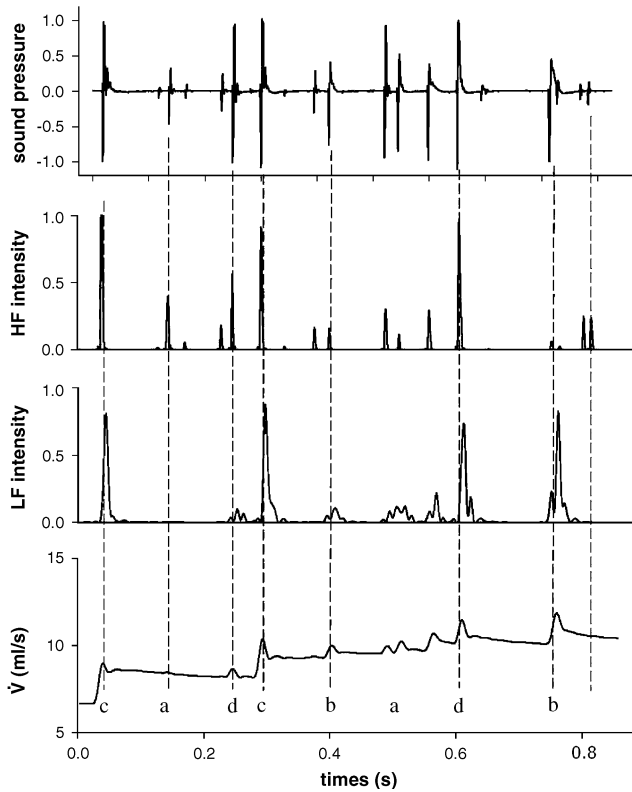
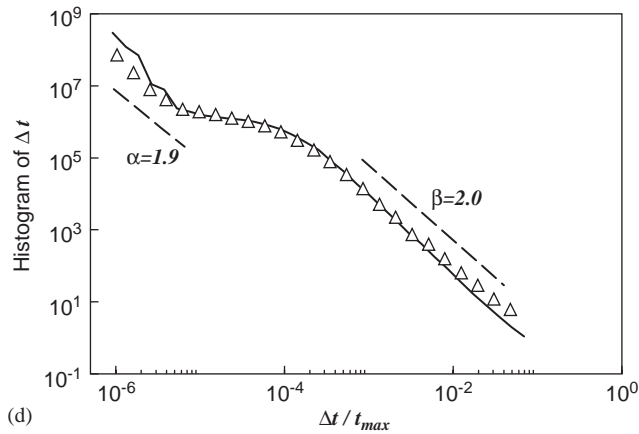
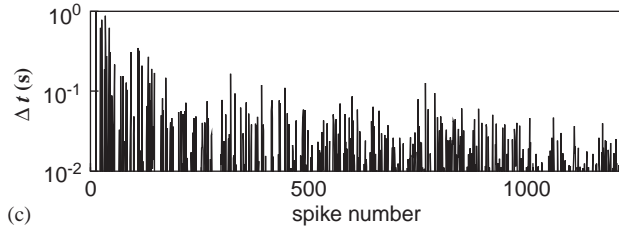
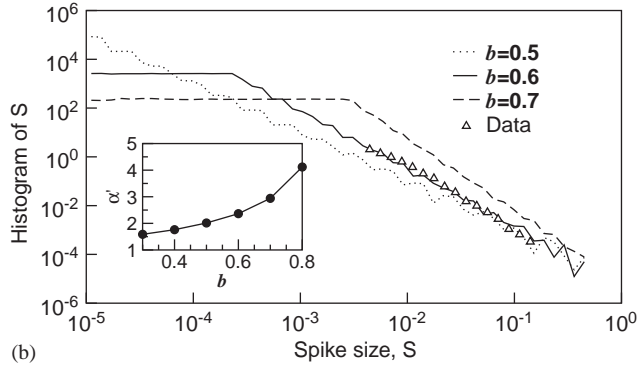
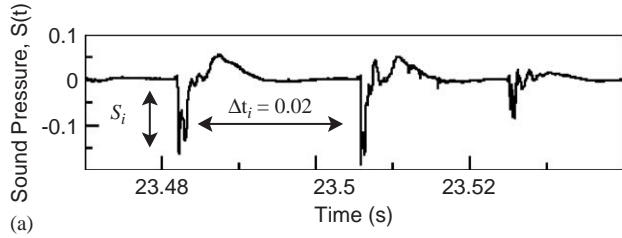


Fig. 1. A segment of crackle (top) and  $\dot{V}$  recording (bottom) during inflation of a lobe. High frequency (HF) and low frequency (LF) sound energy data (in arbitrary units) were computed from high-pass-filtered (1 kHz) and low-pass-filtered (60 Hz) sound intensity, respectively. Note that the individual crackles have different HF/LF energy contents, and the size of a  $\dot{V}$  transient correlates with low frequency energy but not high frequency energy (cf. crackle types a and b). Some  $\dot{V}$  transients are followed by an increased mean flow (c), whereas others (d) are not. If an avalanche does not reach the alveoli, then only airways open and the recorded crackles may not be followed by a measurable  $\dot{V}$  transient because the opened volume is very small. Once an avalanche opens a path from the main bronchus to the alveoli, the corresponding recruited region is immediately available for gas exchange. In this case, the crackles would be followed by a  $\dot{V}$  transient, which also increases the mean level of the  $\dot{V}$  for crackles of type (c).

$\dot{V}$ , transients, in Fig. 1, we magnified a short segment of recording taken from an early phase of inflation where crackles were relatively rare and the transients in  $\dot{V}$  were well separated. It can be seen that every  $\dot{V}$  transient was clearly marked by a crackle or a burst of crackles, whereas not every acoustic event was accompanied by a detectable transient in  $\dot{V}$ . It is also apparent, however, that crackles of similar amplitude may correspond to either a relatively large or a much smaller  $\dot{V}$  transient. By determining the low frequency (<60 Hz) and high-frequency (>1 kHz) components of each crackle, it can be demonstrated that crackles with significant low frequency energy were always associated with detectable transients in  $\dot{V}$ , signifying recruitment of alveoli for gas exchange.



To characterize the statistical features of the crackles, we develop a moving window algorithm that measures the spike size  $S$  in the time series and the time delay  $\Delta t$  between two consecutive spikes (see Fig. 2a). The overall distribution  $\Pi(S)$ , including data from all 12 inflation experiments, follows a power law behavior,  $\Pi(S) \propto S^{-\alpha'}$ , with an exponent  $\alpha' = 2.77 \pm 0.05$  (see Fig. 2b). The time series of  $\Delta t$  values are shown in Fig. 2c. The distribution  $\Pi(\Delta t)$  of  $\Delta t$  (Fig. 2d) shows one pronounced regime of power law behavior,  $\Pi(\Delta t) = \Delta t^{-\beta}$ , with  $\beta = 2.0$  for large  $\Delta t$ , and another  $\Pi(\Delta t) = \Delta t^{-\alpha}$ , with  $\alpha = 1.9$  for small  $\Delta t$ . The large  $\Delta t$  regime is related to the dynamics of distinct avalanches, and the small  $\Delta t$  regime is related to the dynamics of crackles within a single avalanche [6]. The dynamics of distinct avalanches play an important role in the recruitment of closed regions of the lung and will be the main focus of this section.

To understand the power law behavior of  $\Pi(S)$  we develop a model of crackle wave generation and propagation in a tree structure. When the lungs deflate to very low volumes, many peripheral airways close up by forming a liquid bridge between the collapsed airway walls [9]. Experiments on flexible tube models indicate that the opening of a single airway can be characterized by a critical opening threshold pressure  $P_{th}$  [8,14]. If the pressure at the inlet of an airway exceeds this threshold, the airway opens. Thus, we model the airway tree with a binary tree in which a threshold pressure  $P_{i,j}$  is assigned to each airway  $(i,j)$ , where  $i$  is the generation number ( $i = 1, \dots, N$ ) and  $j \in [1, 2^i]$ . We assume that at time  $t = 0$ , all airways are initially blocked. The inflation is simulated by applying an external pressure  $P_E$  at the top of the tree.  $P_E$  is initially assigned the value  $P_{0,0}$ , which is the threshold pressure of airway  $(0,0)$ . Since an airway opens when the pressure in its parent equals or exceeds its critical threshold pressure, the airway  $(0,0)$  now opens and its pressure is set equal to  $P_E$ . Next, the two daughter airways  $(1,0)$  and  $(1,1)$  are checked; if  $P_E > P_{1,0}$  then  $(1,0)$  opens and if  $P_E > P_{1,1}$  then  $(1,1)$  also opens. This process is then continued sequentially down the tree until no airway is found with  $P_{i,j} < P_E$  and defines an avalanche of opening [4]. The inflation is then continued by gradually increasing  $P_E$  in small increments until the entire tree becomes open [5]. When an airway opens a crackling sound wave is generated, and we assume that this sound wave can be represented as a single spike with an amplitude  $S_{i,j}$  proportional to the local threshold pressure  $P_{i,j}$ . A wave traveling up in a daughter branch will be attenuated due to several factors. Here we consider attenuation due to a change in geometry at a bifurcation. Based on the continuity of pressure and volume velocity at the bifurcation, the original pressure spike amplitude  $S_{i,j}$  will be attenuated as  $S'_{i,j} = b_{i,j} S_{i,j}$ , where  $S'_{i,j}$  is the pressure spike amplitude transmitted from the branch



Fig. 2. (a) Magnified segments of  $S(t)$  showing spike amplitudes  $S_i$  and the time intervals between consecutive spikes  $\Delta t_i$ ; (b) the histogram  $\Pi(S)$  of  $S_i$  for 12 inflations (triangles) with  $\alpha' = 2.7$ , and simulations with  $\langle b \rangle = 0.5$  (dots),  $\langle b \rangle = 0.6$  (solid line), and  $\langle b \rangle = 0.7$  (dashed line), in a symmetric binary tree model of  $N = 15$  generations. The inset compares the analytical exponent  $\alpha$ , see Ref. [5] (solid line) and the exponent estimated from the envelope of the distributions (analytical results can be found at Ref. [5]). (c) Linear-log plot of one example of  $\Delta t$ , in seconds, against consecutive spike numbers. (d) The histogram of the interspike intervals for 12 different inflations (triangles). The continuous line is the corresponding histogram of  $\Delta t$  from  $10^4$  simulations in a 14-generation symmetric tree [6].

$(i, j)$  into its parent branch  $(i - 1, j/2)$ . The factor  $b_{i,j}$  is the acoustic attenuation coefficient that depends on the local geometry [5]. We numerically examine how  $\Pi(S)$  and  $\alpha'$  change when  $P_{i,j}$  is uniformly distributed between 0 and 1 and  $b_{i,j}$  has a mean  $b$ . The exponent  $\alpha'$  depends only on  $b$  (see Fig. 2b).

To understand the power law behavior of  $\Pi(\Delta t)$  in Fig. 2b we extend the model. We first note that the lung is inflated by applying an external pressure  $P_E(t)$  at the top of the tree, and uniformly increasing it. Thus,  $P_E(t) = Kt$ , where  $K = P_{\max}/t_{\max}$  is a constant inflation rate. In the model, we rescale both time and pressure so that  $P_{\max} = 1$  and  $t_{\max} = 1$ , thus  $K = 1$ . Since  $P_E$  increases linearly with time, the opening of the root of an avalanche, airway  $(i, j)$ , occurs at time  $t_{i,j} = P_{i,j}$ . Thus, the time difference between the two consecutive avalanches is  $\Delta t_n = \Delta P_n$ , the pressure difference between  $P_E$  values that trigger two consecutive avalanches.

During the time interval  $\Delta t_n$  between two consecutive avalanches  $n$  and  $n + 1$ , the inflation is blocked by the closed airways, the active surface. The closed airways on the active surface have threshold pressures  $P_{i,j}$  that are uniformly distributed between  $P_E(n)$  and 1, where  $P_E(n)$  is the external pressure that has produced the  $n$ th avalanche. The number of closed airways  $N(P_E)$  defines the size of the active surface at each external pressure  $P_E$ . The next avalanche takes place when  $P_E$  becomes equal to the smallest  $P_{i,j}$  on the active surface:  $P_E(n + 1) = \min_{N(P_E)}\{P_{i,j}\}$ . Thus, the time interval  $\Delta t_n$  is defined by  $\Delta t_n = \Delta P_n = \min_{N(P_E)}\{P_{i,j}\}$ , where the minimum is taken over all  $N(P_E)$  closed airways on the active surface. If  $P_{i,j}$  are independent and  $N$  is large enough, then  $\Delta t_n$  is distributed according to an exponential distribution with a mean value of [6]

$$\langle \Delta t \rangle = \frac{1 - P_E}{N(P_E)}. \quad (1)$$

From numerical simulations using the maximum number of generations  $M$  up to 20 and assuming that all segments in the same avalanche opens together, we obtain a single power law where the experimental power law for small  $\Delta t$  is no longer present. To interpret the first power law region of the experimental  $\Pi(\Delta t)$  for  $\Delta t/t_{\max} < 10^{-5}$  (Fig. 2d), we recognize that, when an avalanche consisting of  $s$  openings occurs, the segments in the avalanche do not open simultaneously but are delayed in proportion to the lengths of the segments. We find that the model reproduces the behavior of the experimental data over five decades of  $\Delta t$ . The continuous line in Fig. 2d shows the distribution of  $\Delta t$  for a tree of 14 generations. There are two regions of power law behavior with exponents of  $\alpha = 2.4$  and  $\beta = 2.18$  similar to the experimental values of  $\alpha = 1.9$  and  $\beta = 2.0$  [6].

To further explore the dynamics of the system, the concept of an active surface has been introduced, which consists of the set of branches that are closed but connected to the root of the tree by an open pathway, or the interface between the open and closed regions [6]. Initially, the size of the active surface increases exponentially as the opening of a single branch on the active surface adds two new branches, increasing the size by 1. However, when an avalanche reaches the boundary of the tree, the size of the active surface decreases, becoming zero when all branches are open. The maximum size of the active surface and the pressure at that point

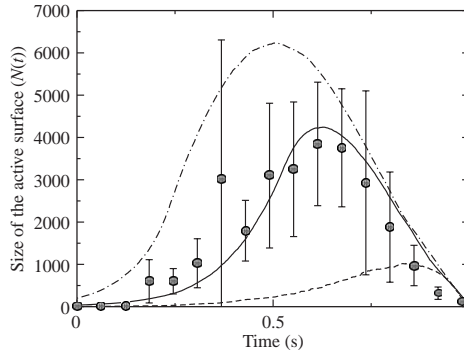


Fig. 3. Experimental and predicted active surfaces. Circles with error bars are the experimental active surfaces obtained from 12 distinct inflations from the collapsed state. The dashed line is the active surface when a random opening pressure threshold is applied, the solid line is obtained with a small generation dependence  $C = 0.01$ , and the dot-dash corresponds to a strong generation dependence  $C = 0.02$ . In all simulated results we used a symmetric tree with 15 generations averaged over 1,000 realizations.

characterize the dynamics of the opening process. It has been found that, in contrast to the distribution of  $\Delta t$ , the active surface is sensitive to the properties of the tree structure as well as the dynamic mechanism of the opening process [7]. Regarding to the opening process the pressure threshold  $P_{i,j}$  in a lung tree is inversely dependent on the diameter  $d$  and proportional to the surface tension  $\gamma_i$  plus a random term,  $P(d) = C\gamma_i/d + \eta$ , where  $C$  is a constant [14,3] and the surface tension  $\gamma_i$  is a function of the surfactant concentration, that is, a function of the generation number  $i$ , since surfactant are produced in the alveolar region.

With regard to physiological implications, we first note that due to the strong attenuation of the crackle amplitudes at successive bifurcations, we only detect crackles down to 14 generations [5,6] which only includes contributions from medium and small sized airways. We suggest that it is possible to reconstruct the evolution of the active surface from experimental data on crackle sound using the relation between the average size of the active surface and the average time interval among crackles. For this purpose, we calculate the average time interval between measured crackles in a non-overlapping moving time window and obtain the average size of the active surface using Eq. (1). The active surfaces thus reconstructed are averaged over data from 12 different inflations. The results, shown in Fig. 3, suggest that the opening pressure thresholds have a weak generation dependence in the lung.

### 3. Discussion

In this paper, we reviewed previous work on the physics of airway opening and recruitment of lung during inflation from the collapsed state. The quantitative agreement between the spike amplitude series from the experiments and simulations

suggests that (i) the irregularities are a consequence of the heterogeneity in the threshold pressures and airway structure of the lung, (ii) the intermittent behavior of the crackle spike time series is due to the avalanche-like opening of the airway segments, and (iii) the scaling behavior observed in the distribution of spike amplitudes is a result of the successive attenuations acting on the sound spikes as they propagate through a cascade of bifurcations along the airway tree.

Similar to the spike amplitude distribution, the time series of inter-crackle intervals measured at the trachea during inflation also shows a complex behavior providing evidence of two separate scaling regions in the distribution of inter-crackle intervals (Fig. 2). The first regime, between time intervals of  $10^{-4}$  and  $10^{-3}$  s, is due to the fact that the avalanche propagation speed is finite. Our numerical simulations suggest that this first power law region is related to the distribution of opening time delays inside the same avalanche and the exponent is likely to be related to the exponent of the airway length distribution [6]. The second regime, between time intervals of 0.1 and 10 s, is due to inter-avalanche timing. This process is related to the propagation of the active surface. It has been shown using mean field calculations that the waiting times between avalanches are distributed according to a power law with an exponent that is close to 2 with a correction factor inversely proportional to the size of the tree [6]. Fig. 2 shows that our numerical model [6] is able to fit the data over a range of five orders of magnitude in inter-crackle intervals.

We have also shown the existence of a close relationship between crackles and the recruited lung volumes available for gas exchange during inflation. This relationship can be studied via simultaneous recording of the pressure–volume curve and the crackle sound. The presence of crackles signify the rupture of the liquid bridge within individual airways which may in turn trigger an avalanche of airway openings. If the opening sequence reaches the alveoli, recruitment occurs.

Our work has potential medical applications. The features of the distribution of crackle spikes as well as the attenuation characteristics of individual crackles may allow the localization of closed airways, and, hence, of local edema or inflammation of tissue. The time interval distribution is useful for studying the transitions between closed and open regions in a diseased lung during breathing. Such a transition can also be accompanied by instabilities along the pressure–volume curves. All these phenomena are related to airway and alveolar collapse and recruitment that occurs in a Cayley-tree. We conclude that recruitment governed by the avalanche-like reopening of airways plays a key role in determining lung function in a variety of conditions including respiratory distress syndrome in premature infants [15], breathing difficulties and attack episodes in severe asthmatics [16], or deteriorated gas exchange in acute lung injury [17].

## Acknowledgements

We thank NSF (BES-0402530) and (OTKA T042971, Hungary) for support.

## References

- [1] E.R. Weibel, *Morfometry of the Human Lung*, Academic, New York, 1963.
- [2] H. Pasterkamp, S.S. Kraman, G.R. Wodicka, Respiratory sounds, advances beyond the stethoscope, *Am. J. Respir. Crit. Care Med.* 156 (1997) 974–987.
- [3] A.M. Alencar, S. Arold, S.V. Buldyrev, A. Majumdar, D. Stamenović, H.E. Stanley, B. Suki, Dynamic instabilities in the inflating lung, *Nature* 417 (2002) 809–811.
- [4] B. Suki, A.L. Barabási, Z. Hantos, F. Peták, H.E. Stanley, Avalanche and power-law behaviour in lung inflation, *Nature* 368 (1994) 615–618.
- [5] A.M. Alencar, Z. Hantos, F. Peták, J. Tolnai, T. Asztalos, S. Zapperi, J.S. Andrade Jr., S.V. Buldyrev, H.E. Stanley, B. Suki, Scaling behavior in crackle sound during lung inflation, *Phys. Rev. E* 60 (4) (1999) 4659–4663.
- [6] A.M. Alencar, S.V. Buldyrev, A. Majumdar, H.E. Stanley, B. Suki, Avalanche dynamics of crackle sound, *Phys. Rev. Lett.* 87 (2001) 088101.
- [7] A.M. Alencar, S.V. Buldyrev, A. Majumdar, H.E. Stanley, B. Suki, Relation between crackle sound and the perimeter growth of a cayley tree: application to lung inflation, *Phys. Rev. E* 68 (2003) 011909.
- [8] D.P. Gaver III, R.W. Samsel, J. Solway, Effects of surface tension and viscosity on airway reopening, *J. Appl. Physiol.* 69 (1) (1990) 74–85.
- [9] D.R. Otis, F. Petak, Z. Hantos, J.J. Fredberg, R.D. Kamm, Airway closure and reopening assessed by the alveolar capsule oscillation technique, *J. Appl. Physiol.* 80 (6) (1996) 2077–2084.
- [10] D.G. Frazer, L.D. Smith, L.R. Brancazio, K.C. Weber, Comparison of lung sound and gas trapping in the study of airway mechanics, *Env. Health Perspect.* 66 (1986) 25–30.
- [11] J.B. Grotberg, Respiratory fluid mechanics and transport processes, *Ann. Rev. Biomed. Eng.* 3 (2001) 421–457.
- [12] R.L.H. Murphy Jr., S.K. Holford, W.C. Knowler, Visual lung sound characterization by time expanded wave form analysis, *New England J. Med.* 296 (17) (1977) 968–971.
- [13] Z. Hantos, J. Tolnai, A.M. Alencar, A. Majumdar, B. Suki, Acoustic evidence of airway opening during recruitment in excised dog lungs, *J. Appl. Physiol.* 97 (2004) 592–598.
- [14] E.T. Naureckas, C.A. Dawson, B. Gerber, D.P. Gaver III, H.L. Gerber, J.H. Linehan, J. Solway, R.W. Samsel, Airway reopening pressure in isolated rat lungs, *J. Appl. Physiol.* 76 (3) (1994) 1372–1377.
- [15] R.E. Pattle, A.E. Claireaux, P.A. Davis, A.H. Cameron, Inability to form a lung-lining film as a cause of the respiratory-distress syndrome in the newborn, *Lancet* 2 (1962) 469–473.
- [16] K.R. Lutchen, D.W. Kaczka, E. Israel, B. Suki, E.P. Ingenito, Airway constriction pattern is a central component of asthma severity: the role of deep inspirations, *Am. J. Respir. Crit. Care Med.* 164 (2001) 207–215.
- [17] J.G. Muscedere, J.B. Mullen, K. Gan, A.S. Slutsky, Tidal ventilation at low airway pressures can augment lung injury, *Am. J. Respir. Crit. Care Med.* 149 (5) (1994) 1327–1334.